Collagen I Self-Assembly: Revealing the Developing Structures that Generate Turbidity

Supporting Material

Jieling Zhu and Laura J. Kaufman*

Department of Chemistry, Columbia University, New York, NY 10027

*corresponding author: kaufman@chem.columbia.edu

Supporting Methods

Microscope Set-up

Figure S1 presents a schematic diagram of the scanning confocal microscope set-up employed for imaging collagen gelation. Except where specified, a 488nm Argon ion laser was used to illuminate samples on a microscope stage equipped with an incubator system (Neue Biosciences). The incubator was pre-warmed and maintained at 27°C, 32°C, or 37°C during collagen gelation. The objective was equipped with a heating ring and also pre-warmed and maintained at the desired temperature during sample gelation. In tri-modal videos, fluorescence and reflected light were collected through a confocal pinhole on two photomultiplier tube (PMT) detectors while light that passed through the sample was collected through a condenser in the forward direction on a third PMT detector. For bi-modal videos where only reflectance and transmittance images were collected, the set-up was identical but PMT 1 in Fig. S1 was not employed.

Images were processed as discussed in Materials and Methods to obtain curves that represented confocal fluorescence microscopy (CFM) total intensity, confocal reflectance microscopy (CRM) total intensity, and *in situ* turbidity (IST) from images collected on PMTs 1, 2, and 3 in Fig. S1, respectively. CRM total intensity and IST curves were used for further data analysis while CFM total intensity was not, as it was dominated by photobleaching.

Supporting Note

Wavelength Dependent Measurements and Data Analysis

Standard Turbidity Measurements

Quantitative information on fiber dimensions may be accessed through wavelength dependent turbidity measurements (1,2). Such measurements were performed on 1.0 mg/ml collagen gels formed at 37°C. First, standard turbidity assays of these gels were performed at 400, 458, 488, 515, 543, and 633 nm (Fig. S3a). From these time scans, wavelength scans were constructed at each time point.

This data was analyzed via

$$\tau\lambda^5 = A\mu(\lambda^2 - Br^2) \text{ with } A = \frac{88}{15}\frac{\pi^3 cn(\frac{dn}{dc})^2}{N_A} \text{ and } B = \frac{92}{77}\pi^2 n^2 \qquad (1)$$

with τ turbidity, λ wavelength of light, μ mass per unit length, c mass concentration of collagen, n the refractive index of the solvent, dn/dc the refractive index increment, N_A Avogadro's number, and r the fibril radius (2). For collagen in water, n = 1.33 and dn/dc = 0.186 g/cm^3 (3). From Eqn 1, plotting $\tau\lambda^5$ vs. λ^2 yields a slope of $A\mu$ and a y-intercept of $-A\mu Br^2$.

Equation 1 assumes the scattering entities are monodisperse rods that are much longer and thinner than the wavelength of light employed (2). These assumptions may break down late in the gelation process at low temperature where fiber bundles are present as well as early in the gelation process at any temperature, particularly before arrest, where long fibers may not be present. Despite these potential problems, analyses of fully formed collagen gels as well as those

undergoing disassembly have been undertaken previously (4,5). In those measurements, as in ours, while Eqn 1 resulted in reasonable mass to length ratios (μ) that changed smoothly during the gelation process, obtained diameter values appeared sensitive to noise and prone to artifacts (4). As such, fibril width was estimated from the mass to length ratio using geometric arguments, with number of molecules in a cross section given by $N = \mu/(M/4.6D)$ with M the molecular mass of the collagen I monomer (290 kDa) and D the axial periodicity seen in banded collagen fibrils (67 nm) (4-6). Given a circular cross-section and measured packing in hydrated fibrils, fibril diameter can be approximated as $d = 1.83\sqrt{N}$ (6). This set of calculations assumes monomer packing that is constant as a function of gelation temperature and throughout the gelation process.

The approach described above was employed on standard turbidity measurements of 1.0 mg/ml collagen gelling at 37°C (Fig. S3a). Plots of $\tau\lambda^5$ vs. λ^2 were well fit by lines both at the end of gelation as well as during the growth phase, as shown in the inset of Fig S3a. Similar fits were obtained for times as early as 2.5 minutes.

Absolute values of $\mu = 8.2 \times 10^{12}$ Da/cm and d = 54 nm were obtained for fully formed 1.0 mg/ml collagen gelled at 37°C using the data shown in Fig. S3a. The value obtained for mass to length ratio is consistent with that measured previously using wavelength dependent turbidity (4,5) and the diameter estimate is also in range of other reports as detailed in the main text.

In Situ Turbidity Measurements

IST and CRM measurements of 1.0 mg/ml collagen gelling at 37°C were also performed at 488, 543, and 633 nm (Fig. S3b). It is apparent that the relative values of IST and CRM intensity were similar as a function of wavelength to those measured via standard turbidity. We note that as at 488 nm (Fig. 3 and Fig. 6 in the main text), CRM preceded IST at early time points, with arrest occurring when a greater proportion of CRM than IST had developed. This was also true at the other wavelengths studied, and no clear trend was found with wavelength.

IST data can be analyzed using Equation 1 in the same manner as standard turbidity data (Fig S3b, inset). Wavelength dependent IST measurements yielded a somewhat lower value of $\mu = 4 \times 10^{12}$ Da/cm. If an effective pathlength of 0.2 mm (compared to the expected pathlength of $\approx$ 0.4 mm based on sample volume and sample cell shape) was employed in converting measured absorption to turbidity, μ obtained from IST was the same as that obtained from standard turbidity measurements. The use of such an effective pathlength may be warranted because a concave meniscus formed in the sample cell creating a smaller effective pathlength ($\approx$ 0.3 mm). The further correction may be warranted due to the tightly focused light used in IST.

Given the relative values of CRM intensity to IST as a function of wavelength (Fig. S3b), it appears that much the same information is present in the CRM intensity and IST results. While no analytical method has been developed to convert CRM intensity to mass to length ratio and diameter, this is in principle possible. Moreover, if CRM intensity is normalized to IST, the analysis described by Eqn 1 can be performed on the normalized CRM intensity measurements and will yield the same results.

Temperature Dependence of Fibril Radius During Gelation

Using the approach outlined above, mass to length ratio and fibril diameter as a function of gelation time were assessed for 1.0 mg/ml gels forming at 37°C and 27°C via wavelength-dependent standard turbidity measurements. Estimating arrest time from CRM

measurements suggests these gels have fibrils of diameter ≈ 20 nm at arrest (Fig. S4). This further supports our description of the network present at the arrest time as a minimal spanning network in which ultimate differential in fibril width as a function of gelation temperature has not yet been established.

Supporting Figures

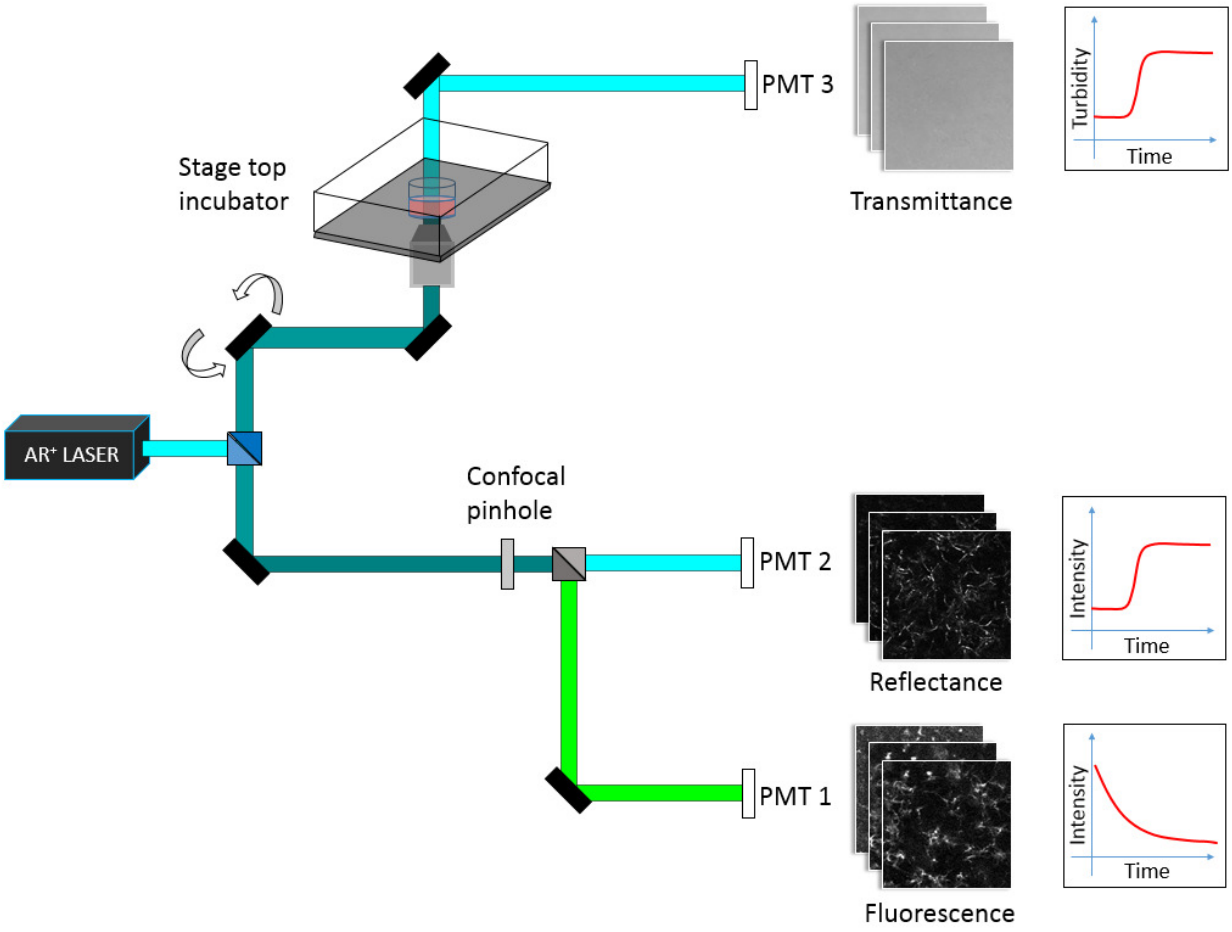

Figure S1. Multi-modal microscopy set-up used for simultaneous collection of scanning transmittance, confocal reflectance, and confocal fluorescence images.

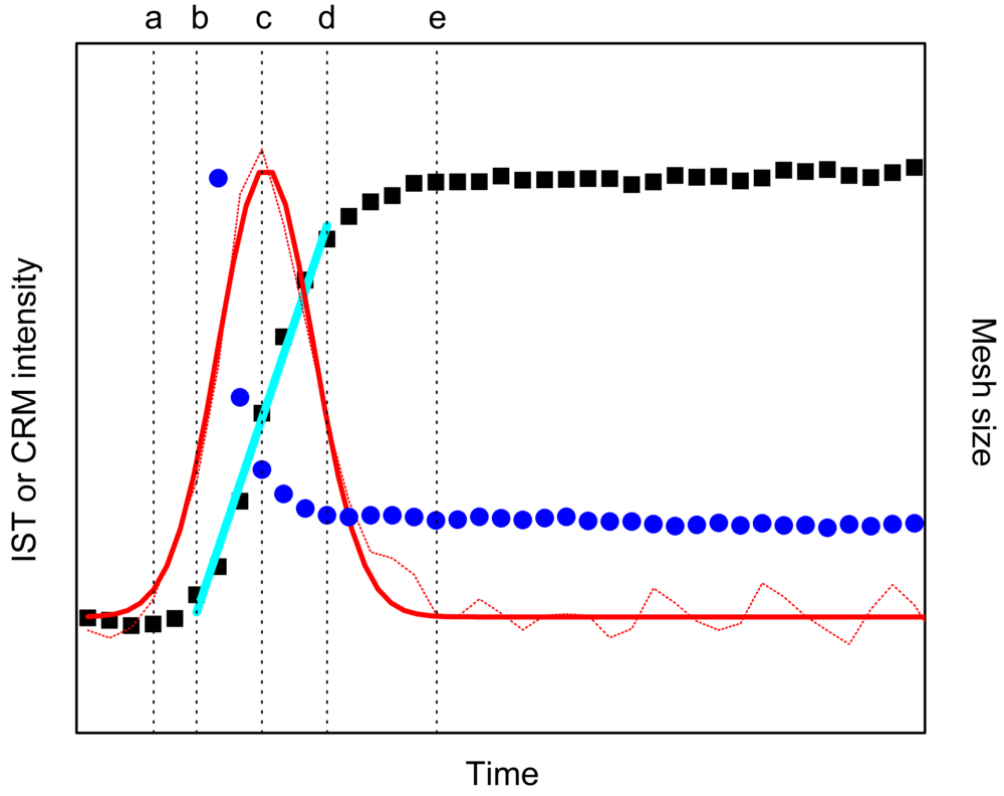

Figure S2. Representative IST curve obtained from a 2.0 mg/ml sample gelled at 37°C (*black squares*). The first derivative (*red dashed line*) and Gaussian fit to the first derivative (*red solid line*) are shown. Mesh size (*blue circles*) evolution is also shown. Relevant variables discussed in the text are (**a**) t_{LAG}, (**b**) t_{ARR}, (**c**) t_{INF}, (**d**) t_{MS}, and (**e**) t_{PL} (indicated by dotted lines from left to right) and slope of growth curve, k_G (*cyan line*).

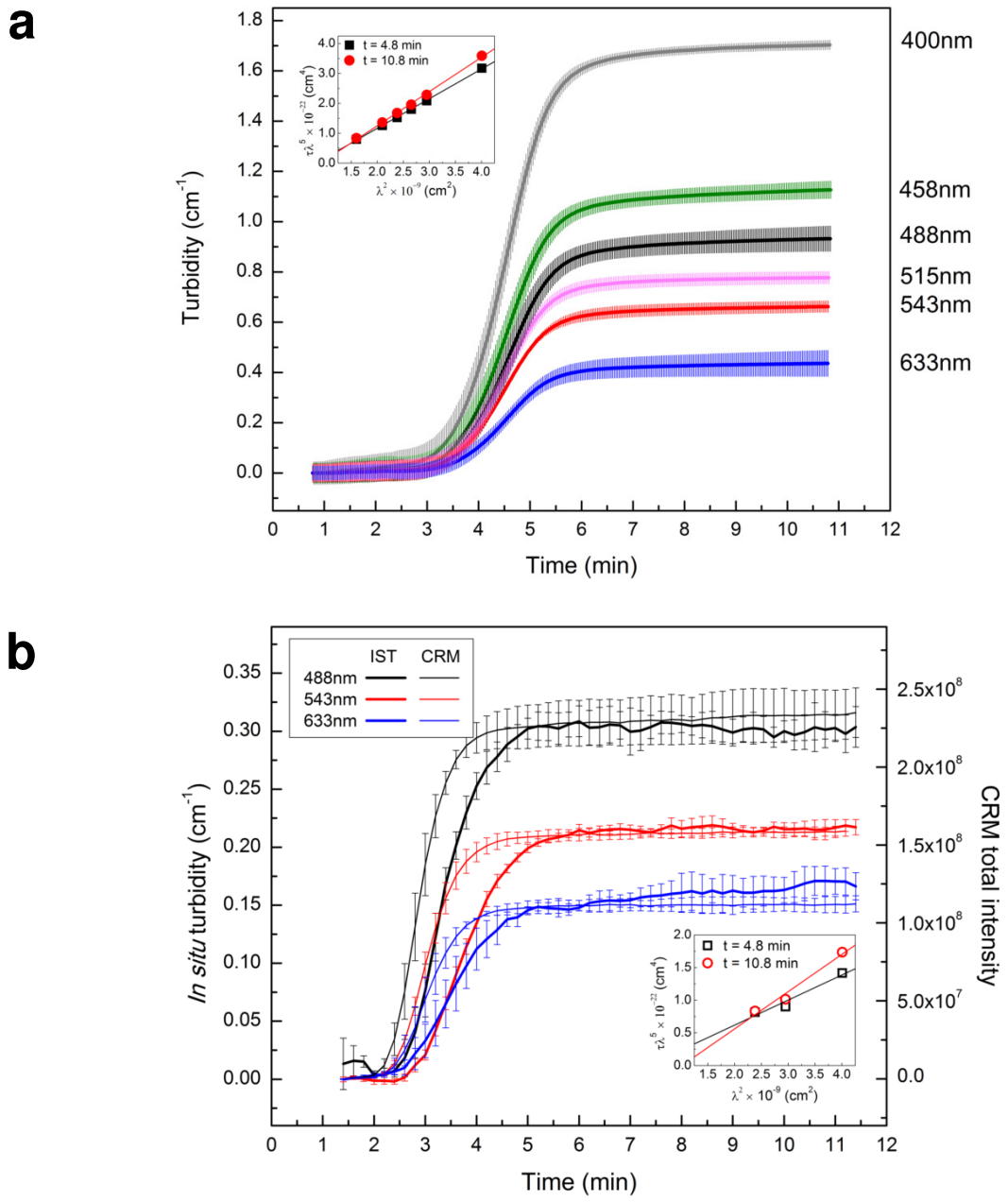

Figure S3. (a) Turbidity curves obtained from 1.0 mg/ml collagen samples gelling at 37°C at, from top to bottom, 400, 458, 488, 515, 543, and 633 nm. (b) IST (thick) and CRM intensity (thin) curves obtained from 1.0 mg/ml collagen samples gelling at 37°C at 488, 543, and 633 nm, from top to bottom. No time shifts of standard turbidity measurements or CRM/IST measurements were performed to account for possible differences in heat transfer between the measurements as described in the main text. In both (a) and (b), average curves were constructed from two to three measurements and error bars are standard deviations. Insets show $\tau\lambda^5$ vs. λ^2 and least squares linear fits for the data reconstructed at t = 4.8. and 10.8 minutes.

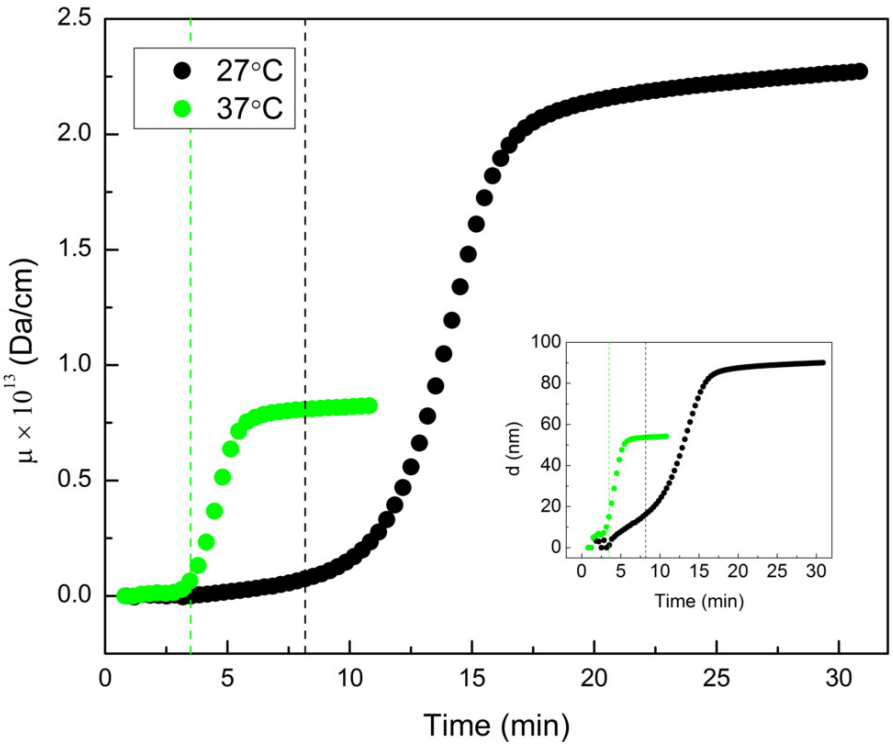

Figure S4. Mass to length ratio and fibril diameter derived from wavelength dependent turbidity measurements of 1.0 mg/ml collagen gelled at 37°C and 27°C. Dashed lines indicate expected arrest times based on CRM imaging and 1 minute shift of standard turbidity measurement compared to CRM/IST measurement as described in Fig. 3 in the main text.

Supporting Table

Supporting Table 1. The ratio of IST to concentration ($A = IST/c$) and that of CRM intensity to concentration ($W = CRM_{int}/c$) at t_{INF} and t_{PL} averaged across temperatures. Time points evaluated were determined from the CRM intensity curve for W and the IST curve for A.

Temperature (°C)	Inflection		Plateau	
	$A \times 10^{-1}$ ± SD	$W \times 10^{8}$ ± SD	$A \times 10^{-1}$ ± SD	$W \times 10^{8}$ ± SD
27	2.1 ± 0.3	1.5 ± 0.1	4.5 ± 0.5	2.9 ± 0.2
32	1.9 ± 0.3	1.3 ± 0.1	3.8 ± 0.4	2.5 ± 0.1
37	1.2 ± 0.1	0.9 ± 0.1	2.5 ± 0.2	1.8 ± 0.2

Supporting Movies

Supporting Movie 1
Fibrillogenesis of 1.0 mg/ml collagen at 32°C recorded by simultaneous time-lapse CFM, CRM, and IST. The channels from left to right are fluorescence, reflectance, and transmittance. Scan speed was 3.26 s/scan, and the interval between images was 10 s. Movies are shown at a frame rate of 10 frames/s. The first 100 images (16.7 min) are shown although the movies were collected for 30 minutes. The movie has been cropped and each image is 91 x 91 μm.

Supporting Movie 2
Fibrillogenesis of 1.0 mg/ml collagen at 27°C, 32°C, and 37°C recorded by time-lapse CRM. The channels from left to right are in order of increasing temperature. Scan speed was 3.26 s/scan, and the interval between images was 10 s (shown at a frame rate of 10 frames/s). The first 150 images are shown for 27°C and 32°C, while 60 images are shown for 37°C since gelation occurred on a much quicker time scale at that temperature. The movie has been cropped and each image is 91 x 91 μm.

Supporting References

1. Carr, M. E. and J. Hermans. 1978. Size and density of fibrin fibers from turbidity. *Macromolecules.* 11:46-50.

2. Yeromonahos, C., B. Polack, and F. Caton. 2010. Nanostructure of the fibrin clot. *Biophys. J.* 99:2018-2027.

3. Brokaw, J. L., C. J. Doillon, R. A. Hahn, D. E. Birk, R. A. Berg, and F. H. Silver. 1985. Turbidimetric and morphological-studies of type I collagen fiber self assembly in vitro and the influence of fibronectin. *Int. J. Biol. Macromol.* 7:135-140.

4. de Wild, M., W. Pomp, and G. H. Koenderink. 2013. Thermal memory in self-assembled collagen fibril networks. *Biophys. J.* 105:200-210.

5. Piechocka, I. K., A. S. G. van Oosten, R. G. M. Breuls, and G. H. Koenderink. 2011. Rheology of heterotypic collagen networks. *Biomacromolecules.* 12:2797-2805.

6. Holmes, D. F. and K. E. Kadler. 2005. The precision of lateral size control in the assembly of corneal collagen fibrils. *J. Mol. Biol.* 345:773-784.